SDC-92-173

DI
T

SDC
SOLENOIDAL DETECTOR NOTES

RADIATION HARDNESS OF DOUBLE-SIDED MICROSTRIP SILICON DETECTOR

T. Ohsugi and M. Kubota
Hiroshima University

H. Miyata and M. Ishizuka
Niigata University

N. Tamura
Okayama University

S. Kobayashi and M. Goto
Saga University

M. Daigo
Wakayama Medical College

Radiation Hardness of Double-Sided Microstrip Silicon Detector

T. Ohsugi and M. Kubota
Department of Physics, Faculty of Science, Hiroshima Univ.

H. Miyata and M. Ishizuka
Department of Physics, Faculty of Science, Niigata Univ.

N. Tamura
Department of Physics, Faculty of Science, Okayama Univ.

S. Kobayashi and M. Goto
Department of Physics, Faculty of Science and Engineering, Saga Univ.

M. Daigo
Wakayama Medical College

Abstract:

Double-sided microstrip detectors based on two different bias feeding methods were fabricated in cooperation with Hamamatsu Photonics Co. for a radiation damage study. The first type utilizes a punch-through method on a p-n junction side and a narrow accumulation layer on an ohmic contact side. The second type uses real resistors made of polycrystalline silicon on both sides. A strip isolation on the ohmic side was attained by a p^+-implantation surrounding an n^+-strip. The radiation damage of those samples was investigated by an irradiation of 65 MeV protons. Up to 20 kGy (2 Mrad), both types of detectors showed good radiation hardness. The bias feeding resistor of the first type, however, significantly degraded above 20 kGy dose. On the other hand, the second type bias feeding resistor maintained the initial resistance stably.

1. Introduction

A silicon microstrip detector is going to be used as an inner part of the SDC central tracker, since it has an excellent position resolution, high rate capability and an excellent two track separation, which are indispensable features for the SSC tracker. The radiation hardness is another critical requirement to the inner tracker, because the inner part of the SDC tracker is expected to be irradiated by the radiation dose of several tens of kGy (Mrad) under the standard SSC luminosity. To minimize a material thickness for a better tracking and calorimetry resolution, a double-sided strip detector is needed for the SDC silicon tracker. In addition, an area of more than 15 m^2 will be covered by the silicon microstrip detector in the SDC tracker. This means that mass production yield should be almost perfect to minimize the cost. After a careful study of these requirements, we concluded that we should develop a double-sided detector with the simplest possible structure as far as the radiation hardness is sufficient. Several types of double-sided microstrip detectors were fabricated for a radiation damage study. One of the main points in this study is to find the best of bias feeding schemes, which is described in terms of "ALEPH-" and "Polysilicon-biasing" in the next section. In this report, we describe the results of the statical and the dynamical measurements of the detector samples irradiated by 65 MeV protons.

2. Detector Samples

In order to test a Double-sided MicroStrip Detector (DMSD), we fabricated various detector samples in collaboration with Hamamatsu Photonics Co. Each sample had a common active area of 6.4x6.4 mm^2, built on a high-resistivity (4 KΩcm) n-type silicon substrate of 300 μm thick. The strip pitch was 50μm.

Two types of bias feeding schemes were investigated in terms of radiation hardness. The first type, which will be referred to as "ALEPH-biasing" hereafter, is the scheme as described in Ref.[1]. The bias voltage is fed to the p^+-strips by an implanted p^+-channel, Bias Ring, which was separated by only 10 μm from each p^+-strip and was surrounding the area of strips as shown in Fig. 1(a). A so-called punch-through effect helps to supply the bias voltage to the strips at the time of depletion process. An illustration of this bias feeding scheme is shown in Fig. 1(b). The bias feeding to the n-strips was made by using a thin and narrow charge accumulation channel between the p-type compensation strips as shown in Fig. 2. The length of the charge accumulation layer was 600 μm, making a resistance of 2 MΩ/layer. We have found a problem in this scheme as described later. As a remedy to this problem, we tried to use a polysilicon resistor instead of a punch-through channel and an accumulation layer, for bias feeding. An insertion of the polysilicon resistor with the length of ~400 μm was made between a bias feeding electrode and each strip at the p-n

junction side as well as at the ohmic contact side. Fig. 3 shows a schematic drawing of such a polysilicon biased double-sided strip detector. The strip structure was made only on one side as in the previous case, while Fig.3 schematically shows structures on both sides. This scheme will be referred to as "Polysilicon-biasing" hereafter. The bias feeding electrode which surrounds the sensitive area is simply connected to each strips by a resistor strip made of polysilicon. These samples had a good uniformity in the polysilicon resistance over the strips area as shown in Fig.4.

We fabricated single-sided samples which have a strip-structure for only on one side of a double-sided detector to investigate the problems of the structures on the p-side and on the n-side, separately. The strip structure of a "p-strip detector" (PSD) was formed by the p^+-implantation strips on the p-side as shown in Fig.1(a) for ALEPH-biasing. The back plane of this sample was a plain n^+-layer. The isolation from adjacent strips is attained by a p-n junction between the p^+-strip and the n-type substrate on the p-side. On the other hand, an "n-strip detector" (NSD) had n^+-implantation strips on the n-side, making an ohmic contact to the substrate. A compensation strip was inserted by p^+-implantation between every neighboring pair of n^+-strips to isolate them from each other as shown in Fig.2(a). No structure was formed on the back plane, p-side, except a plain p^+-layer. The way how the strips are isolated in Polysilicon-biasing case was essentially the same as in ALEPH-biasing case except that an n^+-strip is completely surrounded by a p^+-implantation for the isolation as shown in Fig 3. It is plausible that the accumulated charge at the surface significantly affects the performance of the detector. Especially, the isolation of n-strips is strongly dependent on the depleted region produced by the compensating p-strips, which may be effectively changed from p-type to n-type by the accumulation of electrons. We fabricated two different types of Polysilicon-biasing NSD samples. These samples, named Nb1 and Nb2, had the same structure as the p-strip insertion between the n-strips, but the density of p^+-impurity was different.

The surface of a DMSD is covered in all cases by a thin SiO_2 layer of 0.2 μm thick. Aluminum readout strips are printed on the outer surface of the SiO_2 layer. Signals from these strips are readout to an external instrument either by an AC or a DC coupling mode. The AC coupling readout is in general favorable because it prevents a large leakage current from flowing to an amplifier. The SiO_2 layer served as a coupling capacitor for the AC coupling readout. For the DC coupling readout, a readout strip was connected to an implantation strip through a hole in the SiO_2 layer.

3. Proton Beam Irradiation Test

We have tested the radiation hardness of DMSDs described above by using a 65 MeV proton beam from the AVF cyclotron at Research Center for Nuclear Physics

(RCNP), Osaka University. A proton irradiation gives both a displacement damage in the bulk and an ionization damage on the surface, which is a more realistic experimental condition than any gamma irradiation. The beam intensity was about 1 nA (~10^{10} protons/s) suitable for irradiation with doses up to 60 kGy (6 Mrad) within an hour. The proton beam was once defocussed to obtain good uniformity in space and thereafter collimated, again, at the sample.

The beam intensity was monitored during the irradiation by a Faraday cup. However, the normalization of the irradiation dose was made by utilizing an elastic scattering of proton from carbon. The carbon target of 50 μm thickness was located downstream of the sample, and at the center of a vacuum scattering chamber. The scattered proton was detected at an angle 22.5° to the beam by an NaI counter. A schematic drawing of the setup is shown in Fig. 5. The DMSD samples to be irradiated were mounted on a turn table in the scattering chamber at the suitable position. The sample was located in sequence to the right position on the beam line for irradiation, by turning the table. The beam profile was surveyed by a direct imaging of scintillation light from a ZnS scintillator located at the center of the chamber each time before the irradiation.

4. Static Measurements

(a) Leakage Current

Fig. 6(a) shows a leakage current of the samples before and after the irradiation as a function of the reverse bias voltage. The leakage current for NSD is as low as tens of nano-amperes before the irradiation, while that for PSD is even lower by an order of magnitude. In spite of the difference before the irradiation, the leakage current was almost the same for both cases after the irradiation.

We examined this increase as a function of irradiation dose up to 60 kGy. As Figs. 6(b) and 6(c) indicate, the leakage current is roughly proportional to the dose with an approximate rate of 10 μA/10 kGy(=1Mrad). In another expression, the leakage current is proportional to the fluence ϕ: $I_{leak} = \alpha_p \cdot \phi$, where the leakage current constant α_p is measured in unit of A/cm. In the previous measurement using 12 GeV proton beam [2], the value α_p(12GeV) was measured to be 3×10^{-7} A/cm. In comparison, the value obtained in the present experiment by using a 65 MeV proton beam was α_p(65MeV) = 11×10^{-7} A/cm, and the difference is consistent with the difference in ionizability.

The temperature dependence of the leakage current was also measured (Fig.7). The data was fitted to a function: $I_{leak} = aT^{3/2}e^{-b/T}$, where T is the temperature in Kelvin and the constants are a=9.12×10^{7} (μA·K$^{-3/2}$) and b=0.0754×10^{5} (K).

The leakage current is known to decrease with time. This annealing effect is shown in Fig. 8. It is noted that the effect is seen even after the irradiation dose of 60 kGy.

(b) Strip Isolation

The isolation of the strips was investigated by measuring the inter-strip current by biasing a certain strip relative to the neighboring strips. Fig. 9(a) and Fig. 9(b) show, respectively, for ALEPH-biasing and for Polysilicon-biasing the inter-strip resistance of the p-strip detectors as a function of the reverse bias voltage. The voltage difference between the two neighboring strips was fixed at 1 V. As is expected for non-irradiated samples, the inter-strip resistance increases with the bias voltage, which is explained naturally by the development of depletion region. For the irradiated samples, no significant difference was observed for the inter-strip resistance. However, the resistance was even higher than in no irradiation case, in the lower bias voltage region. In other words, the strip to strip isolation was found to become sightly better after the irradiation. This behavior may be explained by the increase and saturation of the accumulated electrons which prevent the bulk part interfacing to the SiO_2 layer from inversion to the p-type even after the type inversion of the semiconductor occurs. This will be discussed later.

Fig. 9(c) shows the inter-strip current observed in an NSD sample. It is seen that the inter-strip current decreases with the dose after the subtraction of a certain amount of off-set current. This behavior may be explained by the type inversion, which will also be discussed later, of the n-type bulk to the p-type one. If it is the case, better isolation can be expected by realizing a p-n junction around the n^+-implantation.
Fig. 9(d) and 9(e) show the inter-strip resistance for NSDs with the compensating p-strips of different density implantation. The density for Fig. 9(e), Nb2, is more than an order of magnitude higher than that for Fig. 9(d), Nb1. As shown in the figure for the p-side, the isolation by the p^+-implantation of higher density reaches to a plateau at fairly low bias voltages. The full isolation for the lower density case was fulfilled at much higher bias voltage.

In any case, no serious degradation of the isolation was observed either on the p- or on the n-side.

c) Drop of Bias Voltage

This is one of the key points to the present study. Figs. 10 are the voltage difference between each strip and the bias ring plotted as a function of the strip position. In this measurement a bias voltage of 80 V was fed to the bias ring. As shown in Fig. 10(a) which is for NSD samples, the voltage difference around the center

of the sample was as much as 12 V at the irradiation dose of greater than 20 kGy. Even larger voltage drop was observed for PSD samples, as shown in Fig. 10(b), where a voltage drop of about 10 V has to be taken into account even before the irradiation caused by the punch-through effect [1]. The voltage drop was as much as 28 V at 60 kGy. The voltage difference averaged for the strips around the center of each sample is shown in Fig. 11 as a function of the dose. In other words, much higher voltage has to be supplied to the bias ring to get enough voltage at each strip. This may cause a problem of the breakdown at the insulation layer of SiO_2.

On the contrary, the change of the voltage drop for the Polysilicon-biasing was only 500 mV for the NSD, and even smaller for the PSD, up to the dose of 40 kGy as in Fig. 12. This is comparable to the value of 10-30 V for ALEPH-biasing samples. This means that the dramatic improvement of the voltage drops has been achieved by employing the Polysilicon-biasing.

5. Dynamic Measurement

(a) Test by an LED

The type inversion-like phenomenon was observed for the DMSD by injection of the infra-red light from LED. Fig. 13 schematically shows the measurement. In order to observe the behavior of light signal at the depletion of the bulk in progress, we used two different light sources for comparison. They had the mean wavelengths of 850 and of 1150 nm with dispersions of 100 nm. The mean free path of the 1150 nm light in silicon was measured to be ~400 μm, which is longer than the thickness of the sample. On the other hand, the 850 nm light had the mean free path of ~30μm, which means a complete absorption of this light in the sample.

As long as the sample is not fully depleted, the pulse height due to the LED must have a positively increasing relation to the depletion depth through which the light passes. Since the n-type bulk always starts depleting from the p-strip side, the pulse height which is observed by increasing the bias voltage must depend on the side of which the light is injected. An expected behavior is shown also in Fig. 13, where the depleting direction is indicated by an arrow. Fig. 14(a) shows the measured pulse heights as a function of the bias voltage for and undamaged sample. Compared to the data for the 1150 nm light injection, the 850 nm light injected to the p-strip side gave a sufficiently large signal at much below the full depletion voltage.

When the same light was injected to the n-strip side, the situation was reversed, i.e. the signal was much smaller than that for the 1150 nm light. These observations are consistent with what we have expected. On the other hand, the behavior for the irradiated sample, Fig. 14(b), is in contrary to this. It is something like as if the n-type

bulk were switched to the p-type bulk [3]. Such a phenomenon was seen at the irradiation dose above 10 kGy.

A small bump seen at around 40 V is explained to be due to the incomplete isolation of strips while the depletion of the bulk is not completed. In such a case, the charges that have been collected to the readout strip may be more than those collected at the full depletion, because the dimension of a light spot is expected to be sufficiently larger than the size of one strip width.

(b) Test by a β-source

The signal measurement using a Sr-β source was made for the PSD sample, which had been irradiated with the dose of 20 kGy [4]. Before doing this, we have examined the effect of radiation to the shot noise. Figs. 15(a) and 15(b) show the sizes of the total noise for an AC and a DC coupled readout, respectively, as a function of the temperature. The shot noise, which can be estimated by subtracting the constant instrumental noise of about 1,200 e(lectrons) at very low temperatures, increased slightly by the irradiation at the room temperature. The observation was almost the same for both AC coupled and DC coupled readout, but the latter showed somewhat larger noise than the former (1,900 e compared to 1,600 e). The circuit diagram in this measurement is shown in Fig. 16.

As shown in Fig. 17, the shot noise, σ_S, had a relation to the leakage current given by $\sigma_s \propto \sqrt{I_{leak}} \cdot T_s$, with T_S, the shaping time of the amplifier, of 1μs. The source test was employed by measurement of the pulse heights using a pulse height analyzer. We fitted both the pedestal and the β-ray signal distribution to the Gaussian and the Landau distribution, respectively, and obtained each mean value. The pulse height defined here is the difference between the two mean values.

Fig. 18 shows the dependence of the pulse height on the bias voltage. The irradiated sample showed a degradation in the pulse height by about 20 % at 70 V and % at 150 V,respectively, compared with the non-irradiated sample. The signal-to-noise (S/N) ratio was calculated as a function of the temperature. It also showed a degradation to less than a half value at room temperatures for a non-irradiated sample (Fig. 19). The S/N was almost recovered at 0 °C with the relatively high bias voltage of 150 V as shown in the figure. The problem of voltage resistance at the coupling capacitor remains to be fixed in future.

6. Discussion and Conclusions

The test samples of DMSD with a thickness of 300 μm was fabricated and irradiated by a 65 MeV proton beam. The radiation hardness was tested up to the dose of 60 kGy. Through both the statical and the dynamical measurements of the

irradiated samples, the detector concept we have been thinking of was proved to be essentially hard against the radiation. For example, the measurement using the β-source showed that the samples irradiated up to the dose of 20 kGy still had a S/N ratio of 5 even at the room temperature, and this figure can be improved to 9 at 0 °C as shown in Fig. 19.

This number seems to be enough for the actual use of DMSD, since the present dose corresponds to what was estimated after 6 years at the location 15 cm apart from the collision point, assuming that the SSC were operated during 100 days/year at the luminosity of 10^{33} $cm^{-2}s^{-1}$. However, this estimate may be somewhat too optimistic, because the damage effect while the detector is biassed is not taken into account in the present estimate. We have a plan to irradiate biased detectors.

A promising result of the polysilicon resistor gave us a good scope toward the construction of DMSD, while we have to continue the present R&D until enough radiation hardness of DMSD is convinced.

Acknowledgements:

This work has been done in a collaboration with Drs. A. Ando, K. Hatanaka and Y. Mizuno, RCNP, Osaka Univ., K. Inoue and Y. Suzuki, ICRR, Univ. of Tokyo and K. Yamamoto and K. Yamamura, Hamamatsu Photonics Corp. The authors would like to express their sincere thanks for the collaboration.

References:

[1] P. Holl et al., IEEE Trans. Nucl. Sci. 36 (1989) 251

[2] T. Ohsugi et al., Nucl. Instr. Meth. A265 (1988) 105

[3] M. Nakamura et al., Nucl. Instr. Meth. A270 (1988) 42
The type inversion-like phenomena was observed, also, in the neutron irradiation test by the UC Santa Cruz group.

[4] H. Miyata et al., Presented in JPS Meeting, Nara, October 1990

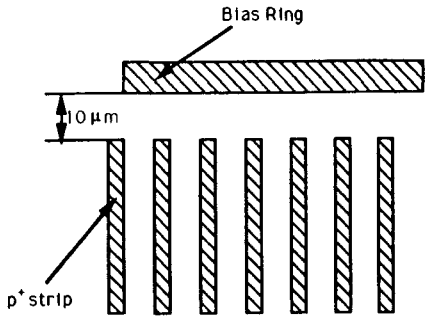

Fig. 1(a)

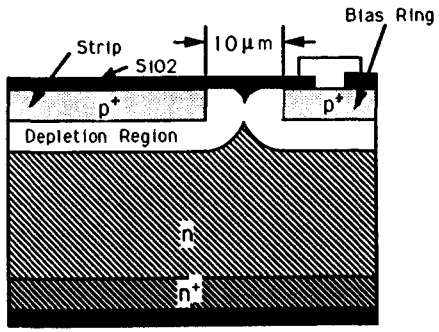

Fig. 1(b)

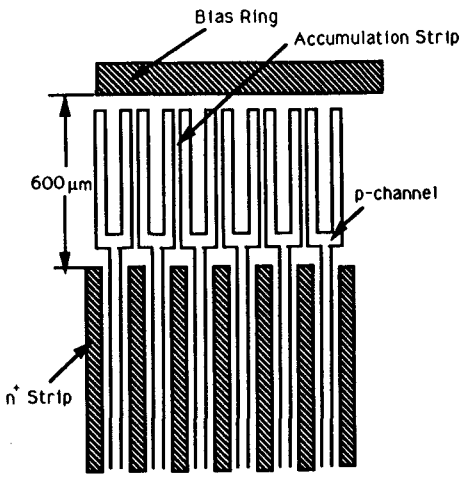

Fig. 2(a)

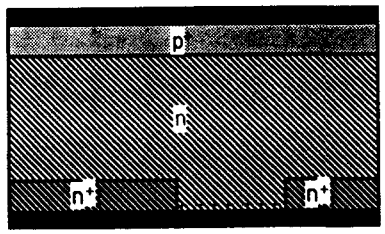

Fig. 2(b)

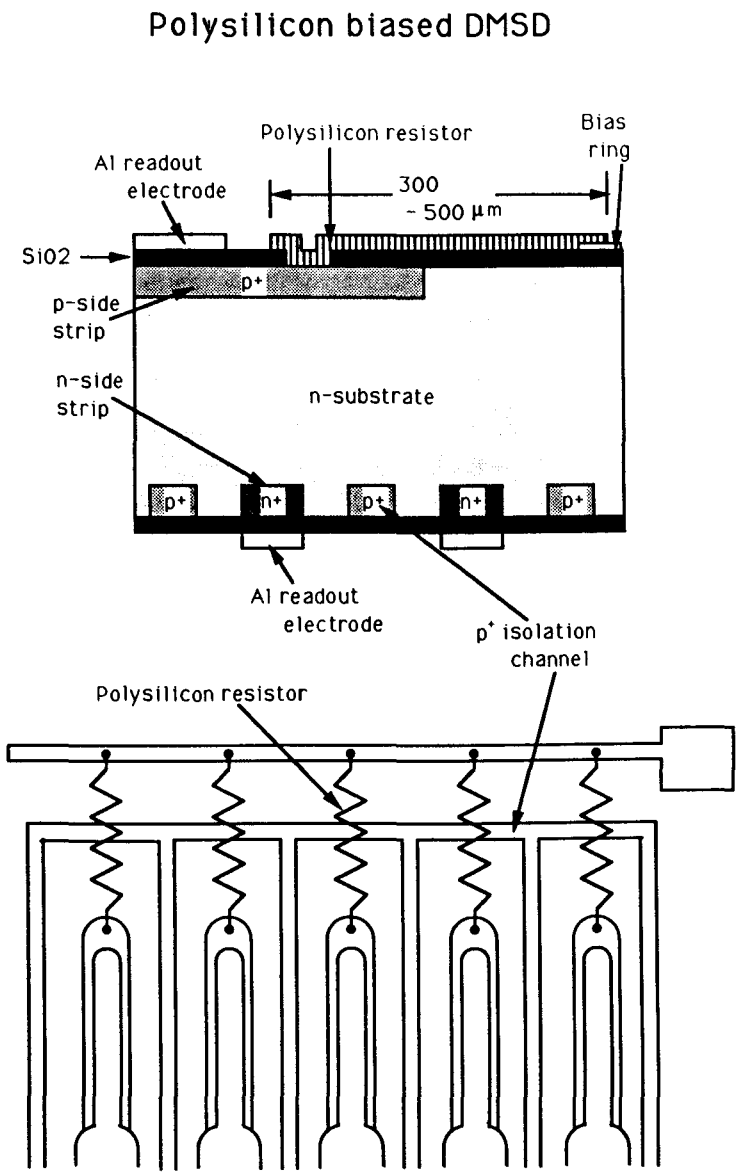

Fig. 3

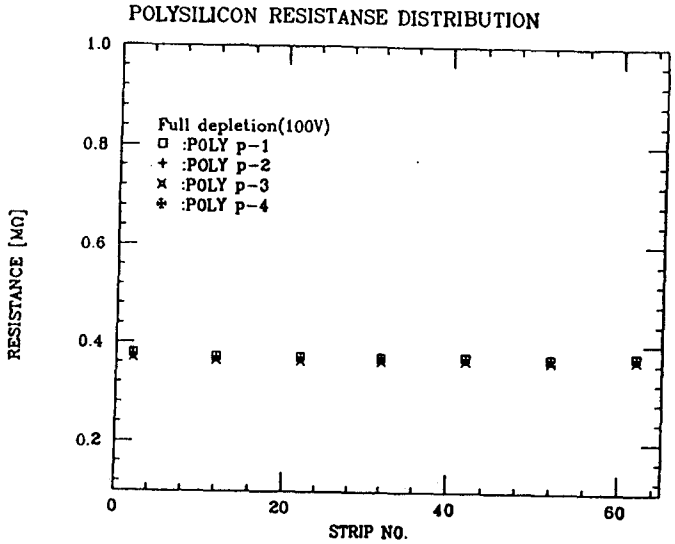

Fig. 4(a)

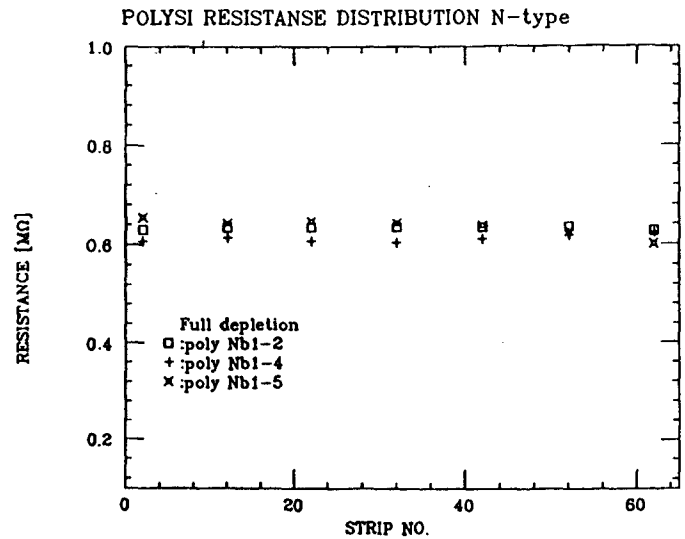

Fig. 4(b)

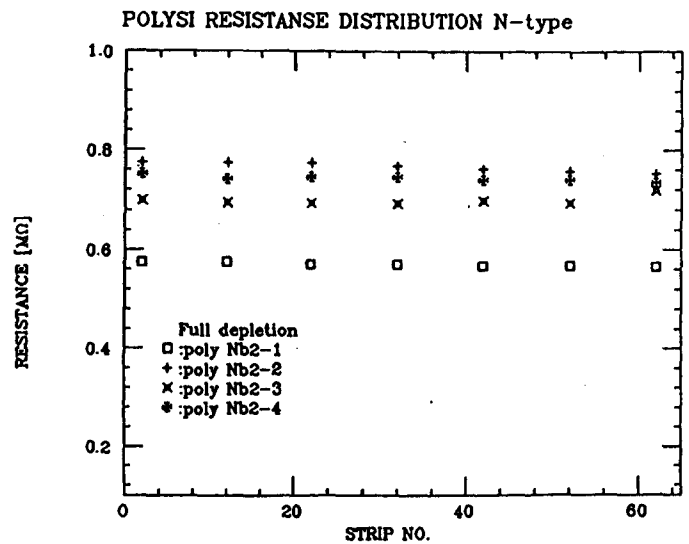

Fig. 4(c)

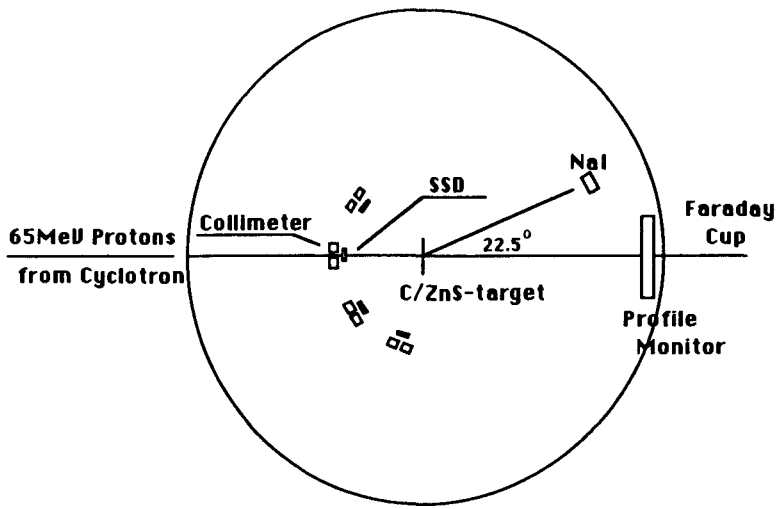
65MeV Protons
from Cyclotron
Collimeter
SSD
NaI
22.5°
C/ZnS-target
Faraday
Cup
Profile
Monitor

Fig. 5

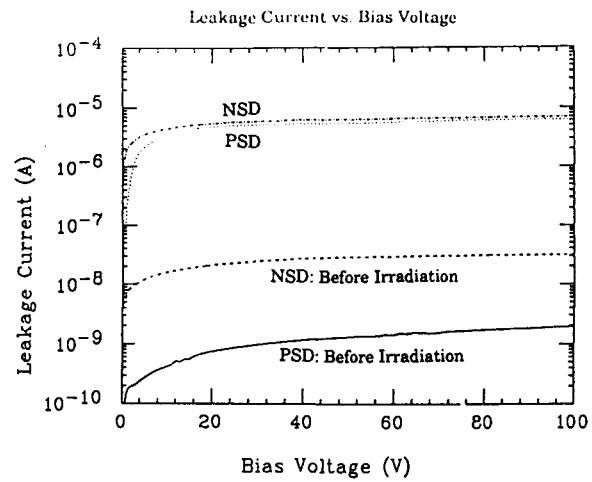
Leakage Current vs. Bias Voltage
Leakage Current (A)
Bias Voltage (V)
NSD
PSD
NSD: Before Irradiation
PSD: Before Irradiation
10^-4
10^-5
10^-6
10^-7
10^-8
10^-9
10^-10
0
20
40
60
80
100

Fig. 6(a)

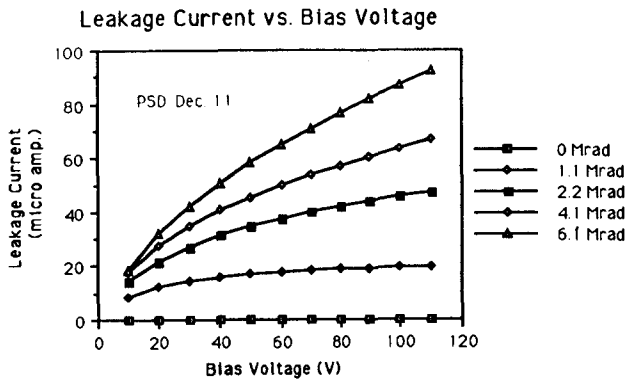

Fig. 6(b)

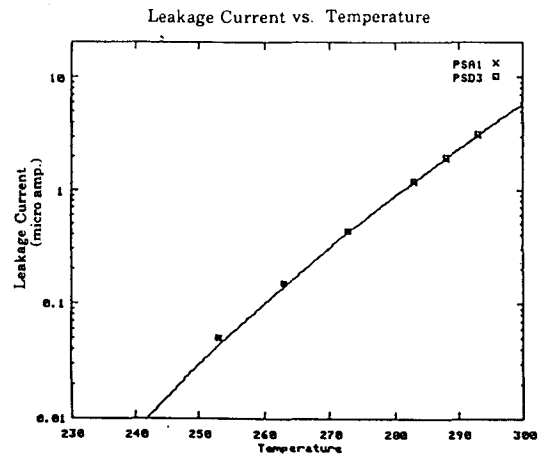

Fig. 7

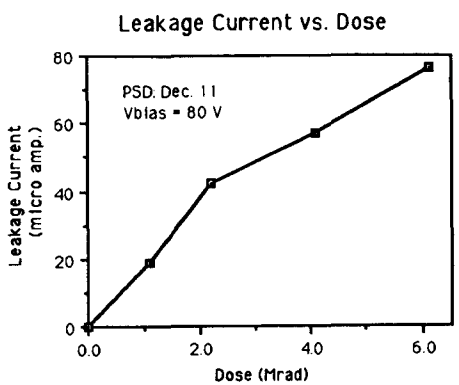

Fig. 6(c)

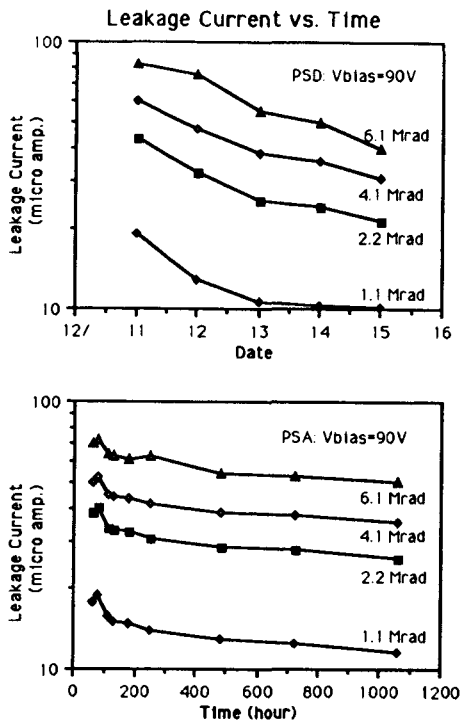

Fig. 8

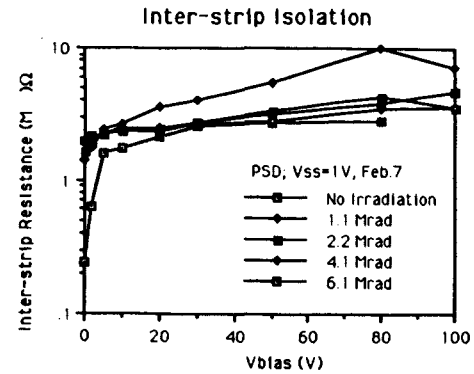

Fig. 9(a)

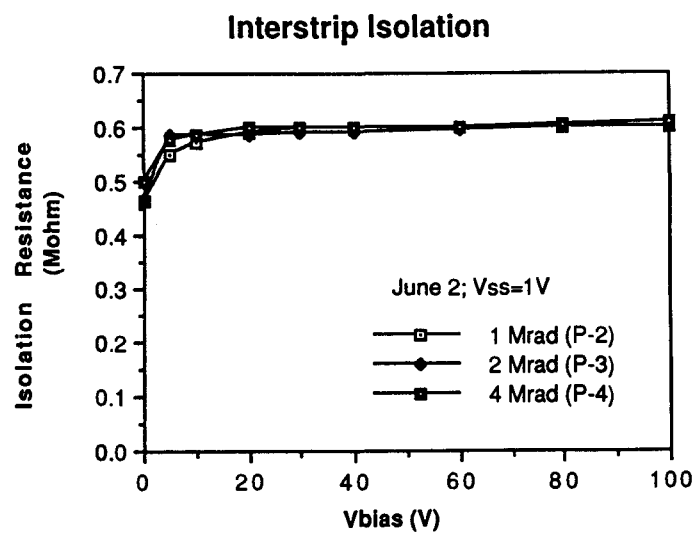

Fig. 9(b)

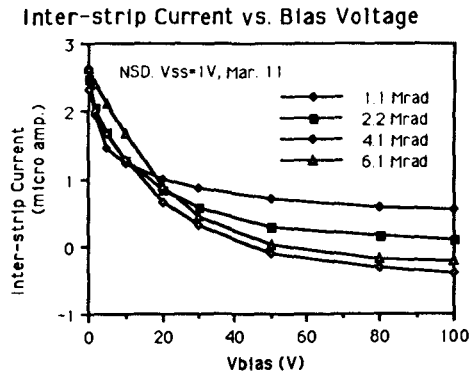

Fig. 9(c)

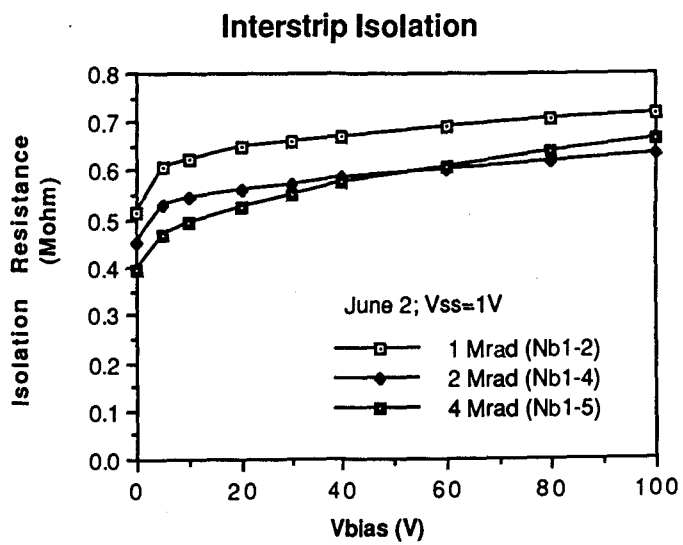

Fig. 9(d)

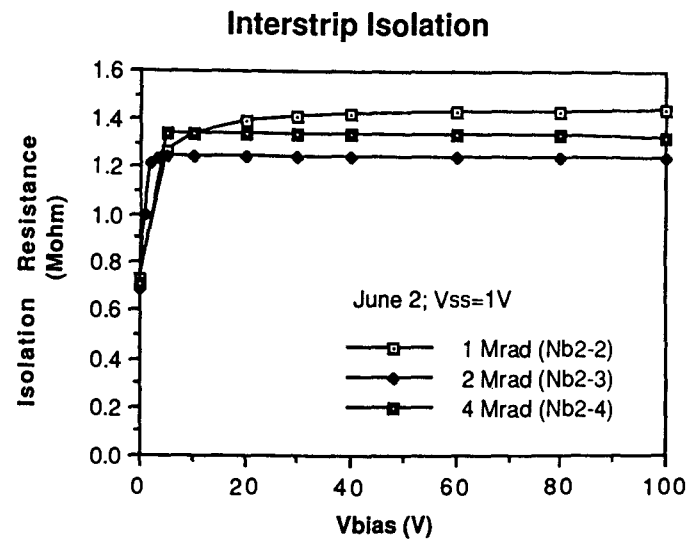

Fig. 9(e)

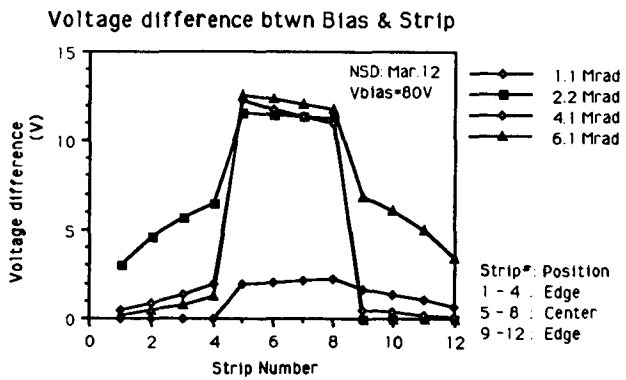

Fig. 10(a)

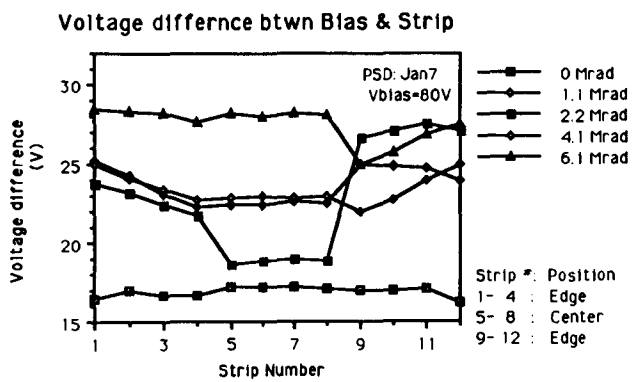

Fig. 10(b)

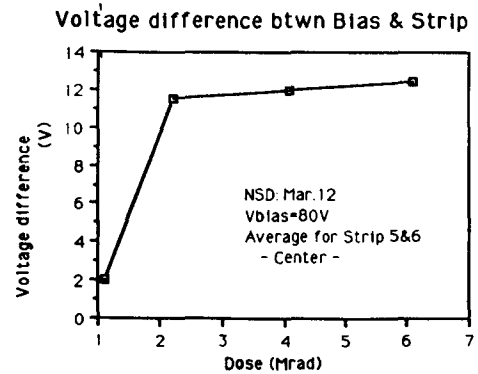

Fig. 11(a)

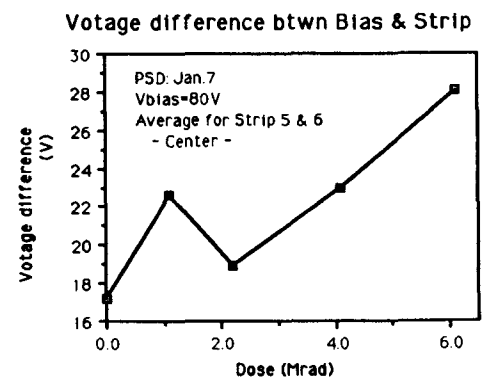

Fig. 11(b)

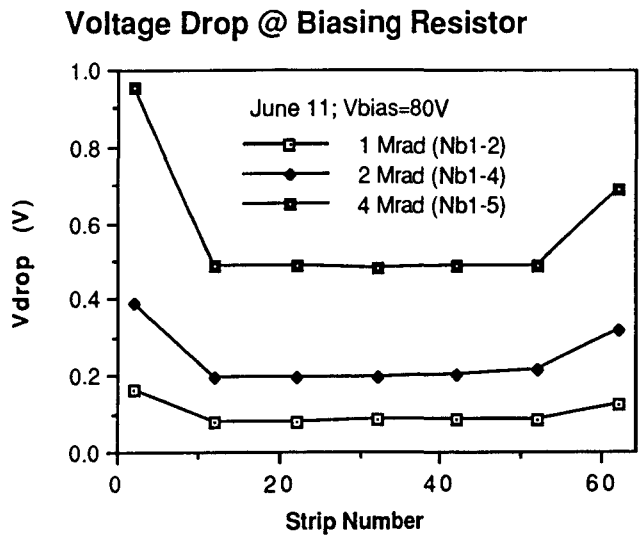

Fig. 12(a)

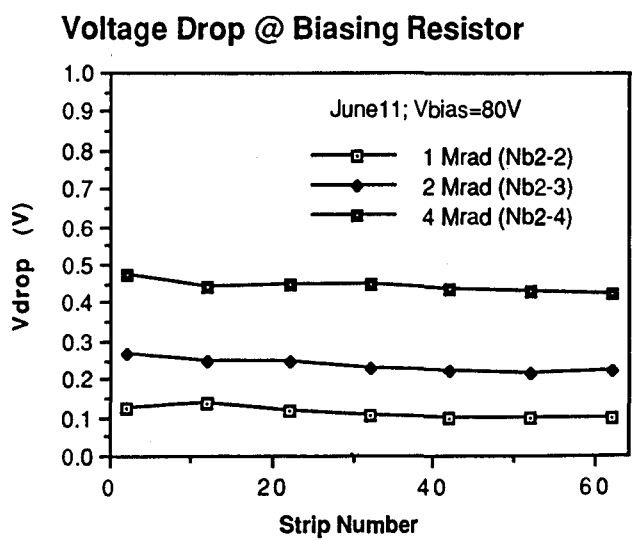

Fig. 12(b)

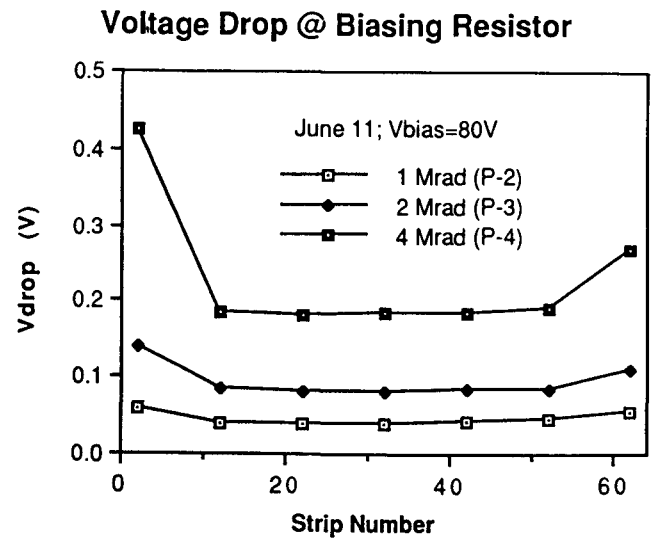

Fig. 12(c)

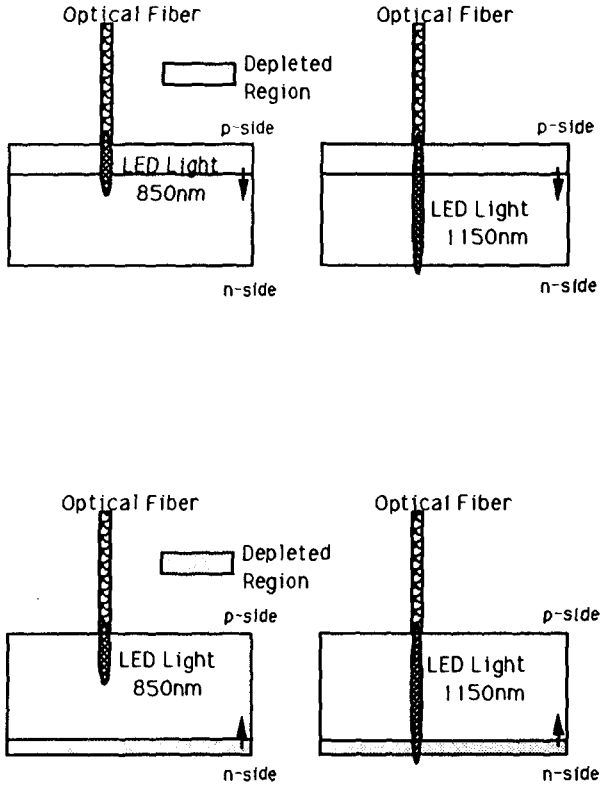

Fig. 13

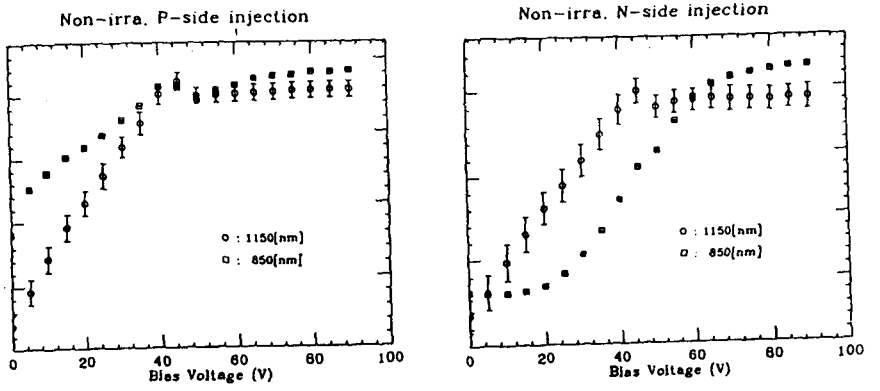

Fig. 14(a)

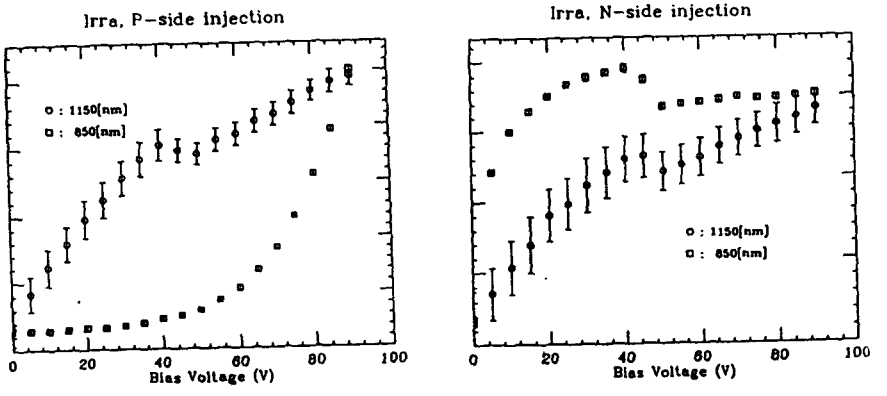

Fig. 14(b)

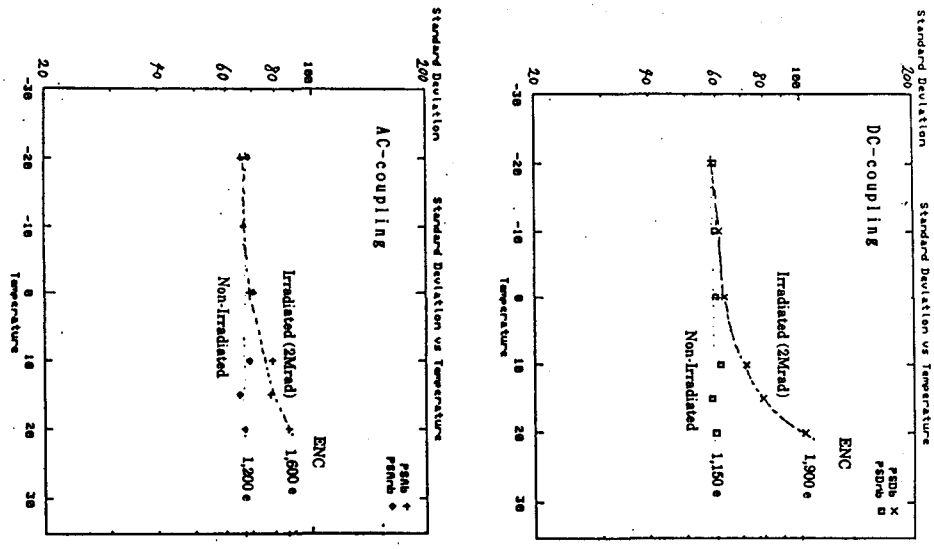

Fig. 15

Logic Diagram for SSD Trigger

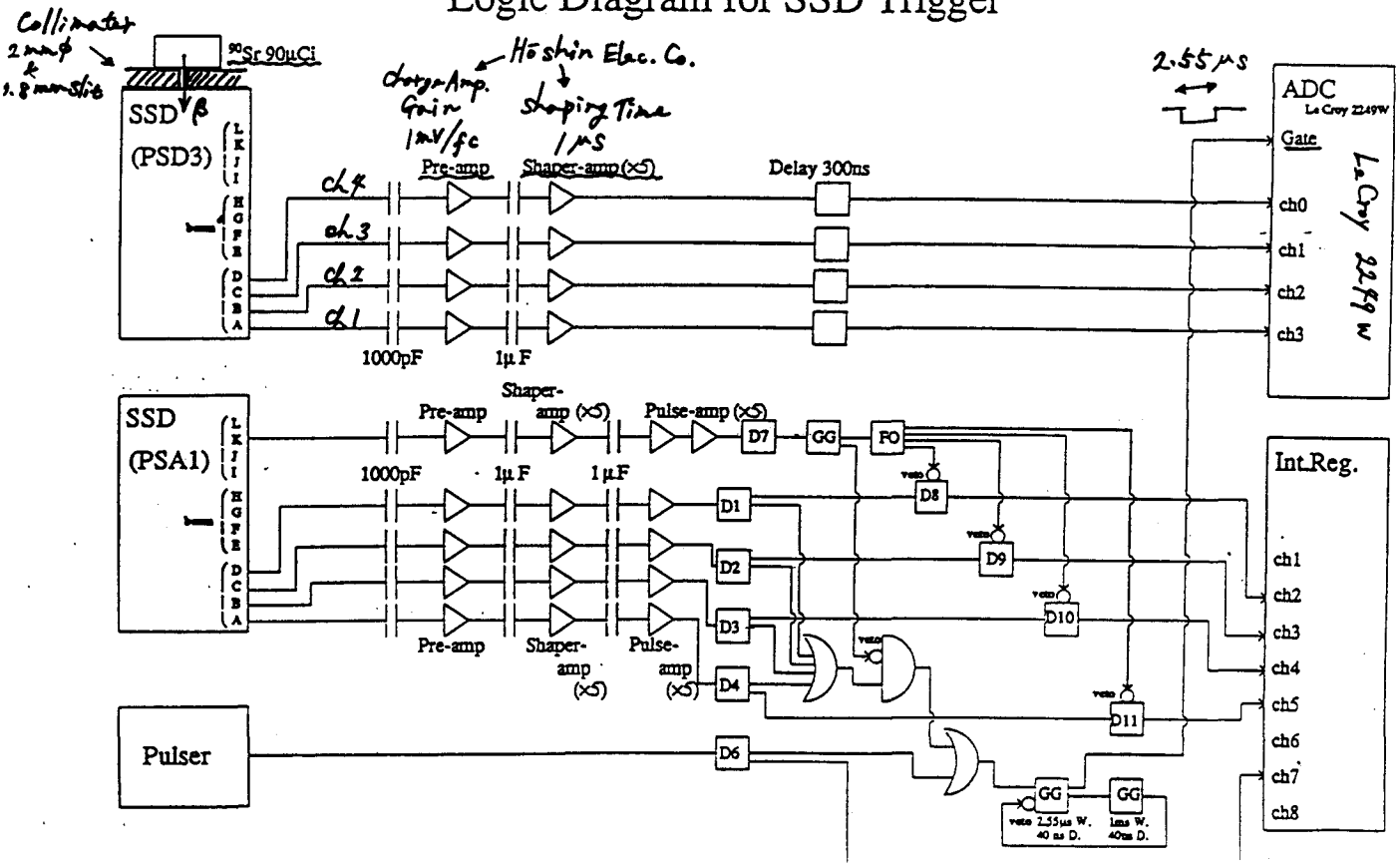

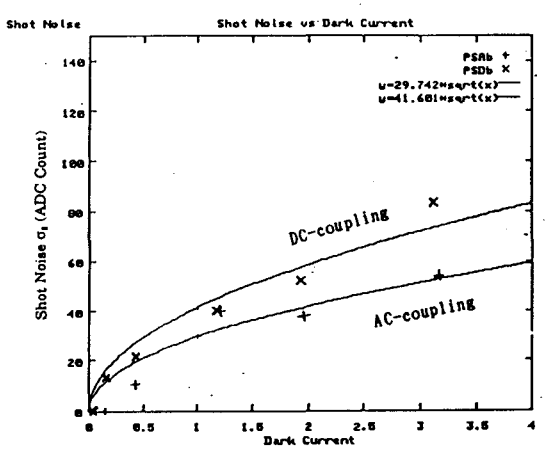

Fig. 17

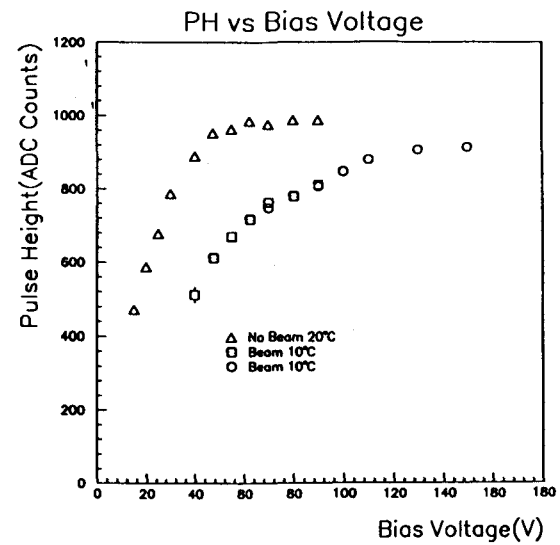

Fig. 18

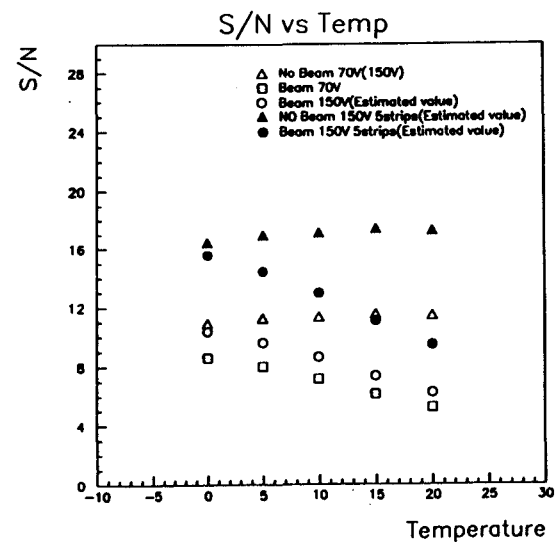

Fig. 19